Int. J. Electrochem. Sci., 13 **(2018)** 7643 – 7654, doi: 10.20964/2018.08.65

International Journal of
ELECTROCHEMICAL
SCIENCE
www.electrochemsci.org

Amperometric Sensing of Paracetamol Using a Glassy Carbon Electrode Modified with a Composite of Water–Stable Metal−Organic Framework and Gold Nanoparticles

Yifei Shi[1,2], *Yubin Zhang*[1,2], *Yang Wang*[1,2], *Huayu Huang*[1,2,*], *Junjie Ma*[1,2]

[1] Shaanxi Key Laboratory of Earth Surface System and Environmental Carrying Capacity, Northwest University, Xi'an 710127, China
[2] College of Urban and Environmental Science, Northwest University, Xi'an 710127, China
[*]E-mail: huanghy@nwu.edu.cn

Received: 7 April 2018 / *Accepted:* 6 June 2018 / *Published:* 5 July 2018

A paracetamol electrochemical sensor was facilely fabricated by modifying a glassy carbon electrode (GCE) with a water–stable metal−organic framework (MOF) and gold nanoparticles (AuNPs). The MOF/AuNP composites were synthesized by hydrothermal and sonication methods. The MOF possesses a high specific area and coordinatively unsaturated sites as an amplification element, and the AuNPs can amplify the electrochemical signal with excellent conductivity intensity. The modification activity of the MOF/AuNP composites was investigated via voltammetric determination of paracetamol. A sensitive paracetamol measurement method was built using the MOF/AuNP modified GCE. The oxide peak response changed linearly as the paracetamol concentration increased from 0.01 nmol L^{-1} to 100 μmol L^{-1}, and the low detection limit was 0.0011 nmol L^{-1} (3σ). The present work offers a new method to analyze paracetamol in tablets and expands the application of MOFs in the electrochemical field.

Keywords: Nanomaterial; Electrochemical Sensor; Acetaminophen; Pharmaceutical analysis

1. INTRODUCTION

Paracetamol, one of the most common analgesic and antipyretic drugs, is widely used as a common pain killer in pregnant women and during childbirth [1]. However, the toxicity of paracetamol cannot be ignored. Fan showed that the risk of childhood asthma may be increasing exposure to paracetamol during the first trimester of pregnancy [2]. Additionally, paracetamol is also considered an endocrine disruptor after subchronic exposure [3]. With increasing public awareness of human health and environmental preservation, it is highly desirable to establish analytical methods for the

determination of paracetamol. To date, there are many reported methods to characterize paracetamol, including spectrophotometry [4], liquid chromatography [5], ultraviolet spectrophotometry [6] and capillary electrophoresis [7]. However, these methods are highly specialized research tools. Many of these methods require a complicated pretreatment process, and thus the analysis of paracetamol takes a considerable amount of time and is expensive and laborious. Fortunately, low−cost and high−sensitivity electrochemical methods have been considered to detect paracetamol in real samples [8]. Paulo used Printex 6L carbon nanoballs to fabricate a chemical sensor for paracetamol determination with a limit of detection (LOD) of 8.0 nmol L^{-1} [9]. Kutluay's group prepared an electrochemical sensor using carbon nanotube and cobalt nanoparticles to detect paracetamol [10]. Li fabricated a paracetamol electrochemical sensor using Pd/graphene oxide nanocomposite with an LOD of 2.2 nmol L^{-1} [11]. Therefore, it is advisable to use an electrochemical method due to the advantages and tremendous development potential for the determination of paracetamol.

Nanomaterials have received attention throughout the world for several decades and have been widely used to modify electrodes for electrochemical sensing. A metal−organic framework (MOF) is a nanoporous polymeric material of a crystalline solid with a typical structural and functional diversity [12]. An MOF possesses an ultrahigh specific area, high chemical stability, adjustable surface functionality and coordinatively unsaturated sites [13]. MOFs have been used in electrochemical sensing studies because of their unsurpassed versatility and performance. The combination of zirconium−based MOF and mesoporous carbon has been used for sensitive detection of dihydroxybenzene isomers [14]. MOF−graphene composites have been used to modified electrodes by electrodeposition to detect catechol and hydroquinone [15]. However, the applications of MOF in electrochemistry are limited due to their poor electron−conductive properties [16]. Among the various ways to improve the sensing performance of a sensor, doping with noble metals, especially nanonoble metals, is an efficient method. Gold nanoparticles (AuNPs) have excellent conductivity, catalytic ability and biocompatibility [17] and often function as key factors in catalysis [18] and sensors [19,20]. Graphene and Fe_3O_4/AuNPs amplify the electrochemical response for carcinoembryonic antigen detection and result in an LOD of 0.39 pg mL^{-1} [21]. Zhai and coworkers developed an electrochemical sensor with Au−Ag nanoparticle/multiwalled carbon nanotubes−sulfonated graphene to detect mangiferin and icariin and obtained a low LOD of 0.017 μmol L^{-1} for both compounds [22]. Loading AuNPs onto a nanomaterial surface can greatly enhance the sensing and catalytic properties. Mixing an MOF and AuNPs is a bolder but effective strategy to enhance the conductivity of MOFs and can broaden their use in electrochemical applications. Silva synthesized AuNP@MOF composites and immobilized them on carbon paste electrodes and determine bisphenol A with an LOD of 37.8 μmol L^{-1} [23]. Hosseini used Au−SH−SiO_2@Cu−MOF to fabricate a hydrazine electrochemical sensor with a detection limit of 0.01 mol L^{-1} [24]. Actually, an excellent synergistic increase in the electrocatalytic activity and electrochemical performance was achieved by combining the benefits of an MOF and AuNPs. A major challenge of MOFs in water treatment is to enhance their stability in aqueous media.

Herein, we synthesize composite materials consisting of copper MOF and AuNPs. A water−stable copper MOF was prepared through a hydrothermal method, and AuNPs were introduced to modify the MOF by rapid sonication to enhance the electron transfer property. A Nafion ionomer was added to the MOF/AuNP composites as a physical binder and a safeguard of the glassy carbon

electrode (GCE) [25]. A paracetamol electrochemical sensor was fabricated using MOF/AuNPs and Nafion. The electrochemical response was greatly amplified owing to paracetamol adsorption on the MOF surface and the excellent electrocatalysis of AuNPs. Furthermore, the developed electrochemical sensor was employed for the pharmaceutical analysis of paracetamol in tablets.

2. EXPERIMENTAL

2.1. Materials and apparatus

Paracetamol was purchased from Sigma−Aldrich (USA). Sodium tetrachloroaurate tetrahydrate ($HAuCl_4 \cdot 4H_2O$), copper nitrate trihydrate [$(CuNO_3)_2 \cdot 3H_2O$], sodium citrate and benzene−1,3,5−tricarboxylic acid (BTC) were purchased from Aladdin (Shanghai, China). Deionized water was prepared from a Millipore unit (Bedford, MA, USA). Different pH phosphate buffers (0.1 mol L^{-1}) were prepared by mixing NaH_2PO_4 (0.1 mol L^{-1}) and Na_2HPO_4 (0.1 mol L^{-1}) solutions.

Morphology characterizating including scanning electron microscopy (SEM) and transmission electron microscopy (TEM) was conducted on a Sigma 300 microscope (ZEISS, Germany) and a Tecnai F30G2 microscope (FEI, Netherlands), respectively. X−ray powder diffraction (XRD) patterns were measured on a D8 ADVAHCL (Bruker, Germany) instrument using Cu Kα radiation. The ultraviolet–visible (UV−vis) absorption spectra were obtained using an Aquamate spectrometer (Thermo Fisher Scientific, USA). Paracetamol was analyzed at 25 ℃ in a high-performance liquid chromatography (HPLC) system equipped with a 2695 Separations Module and a 2489 UV–Vis detector (Waters, Mildford, MA, USA). The separation stationary phase was a C_{18} column (4.6 mm×150 mm, 5 μm, Phenomenex, USA). The mobile phase was a mixture of ammonium acetate buffer (pH 6.0, 10 mM) and acetonitrile (95:5, v/v), and the flow rate was 1 ml min^{-1}. The analyte was monitored at 243 nm. The injection volume was 20 μL in the HPLC measurement.

2.2. MOF and AuNPs Preparation

The MOF was synthesized with a modification of a previously reported methodology [26]. $(CuNO_3)_2 \cdot 3H_2O$ (24.1 mg), BTC (21 mg), CH_3CH_2OH (5 mL) and H_2O (5 mL) were mixed under magnetic stirring for 30 min. The mixture was kept in a Teflon stainless steel vessel at 120 °C for 3 days. The blue powder (MOF) was obtained after the reactor was cooled to room temperature. The MOF (1 mg) was dispersed in one milliliter of ethanol, and the dispersion was sonicated and stored at 4 °C.

AuNPs were prepared and characterized following the reported method [27]. First, 1.5 mL of sodium citrate (1%, m/*v*) was added to 48.5 mL of deionized water, and the solution was heated to 100 ℃. Five−hundred microliters of $HAuCl_4$ (1%, m/*v*) was added to the boiling solution, and the solution was maintained at 100 ℃ for 30 min. After cooling to room temperature, the AuNPs were concentrated via centrifugation for 20 min at a speed of 10,000 rpm. The pellet was dispersed in 2 mL of water after removing the supernatant.

2.3. Preparation of the MOF/AuNPs GCE

The GCE was polished with 0.05 μm alumina powder, and ultrasonically cleaned with deionized nitric acid (50%, *v*/*v*), ethanol and water. The MOF/AuNP composites were prepared by mixing well−dispersed MOF−ethanol and the same quantity of an AuNP suspension, and sonicating the mixture for 5 min with 10 μL of Nafion (0.01%). Subsequently, the suspension was cast on the GCE surface and dried in air.

2.4. Analytical procedure

The electrochemical experiments were performed on a CHI 660E electrochemical workstation (Chenhua, China). A 3 mm bare or modified GCE was used as the working electrode. A platinum wire was applied as the counter electrode. A Ag/AgCl electrode was used as the reference electrode. Differential pulse voltammetry (DPV) was recorded from −0.6 to 0.4 V. The increment step was 1 mV, the amplitude was 50 mV, and the pulse period was 0.2 s.

3. RESULTS AND DISCUSSION

3.1. Characterization

To demonstrate the preparation of the MOF/AuNPs, the morphologies, microstructures and size of the samples were examined by SEM and TEM. Fig. 1A shows, an MOF SEM image that displays the quintessential micron−sized crystal structure in accordance with previously reported descriptions [28]. Moreover, the MOF appears to exhibit parallelogram−shaped particles with sizes of several 500 nm in Fig. 1B. A TEM image of the AuNPs is displayed in Fig. 1C, and the morphology of small quasi−spherical nanoparticles with diameters of 16 ± 1 nm is observed. The TEM image of the MOF/AuNPs (Fig. 1D) shows that, the surfaces of the MOF were decorated by a large amount of AuNPs that appear to be black dot−like objects. In addition, there is no obvious aggregation or morphological changes after loading AuNPs on the MOF surface.

An XRD pattern of the MOF is shown in Fig. 2A. The XRD pattern was consistent with that of a simulated XRD pattern of the MOF, confirming the phase purity of the synthesized MOF [29]. The twelve peaks are observed at 9.6°, 11.6°, 13.5°, 14.7°, 16.4°, 17.5°, 19.0°, 20.1°, 26.0°, 29.3°, 35.3° and 39.1° for diffraction angles (2θ) from 5 ~ 50°, and the results are similar to the reported data [30]. Fig. 2B shows the UV–vis spectra of the MOF, AuNPs and MOF/AuNPs recorded over the wavelength range of 400 to 1000 nm. There is a well–defined peak for the AuNPs at 521 nm [31], and the absorption peak of the MOF emerges at approximately 712 nm. The UV–vis spectrum of the MOF/AuNPs exhibits the same absorption bands as that of the AuNPs, suggesting that the AuNP composites were stable. However, the location of the MOF displays a slight blueshift owing to the excitation of surface plasmon vibrations, confirming the interaction of the MOF and AuNPs.

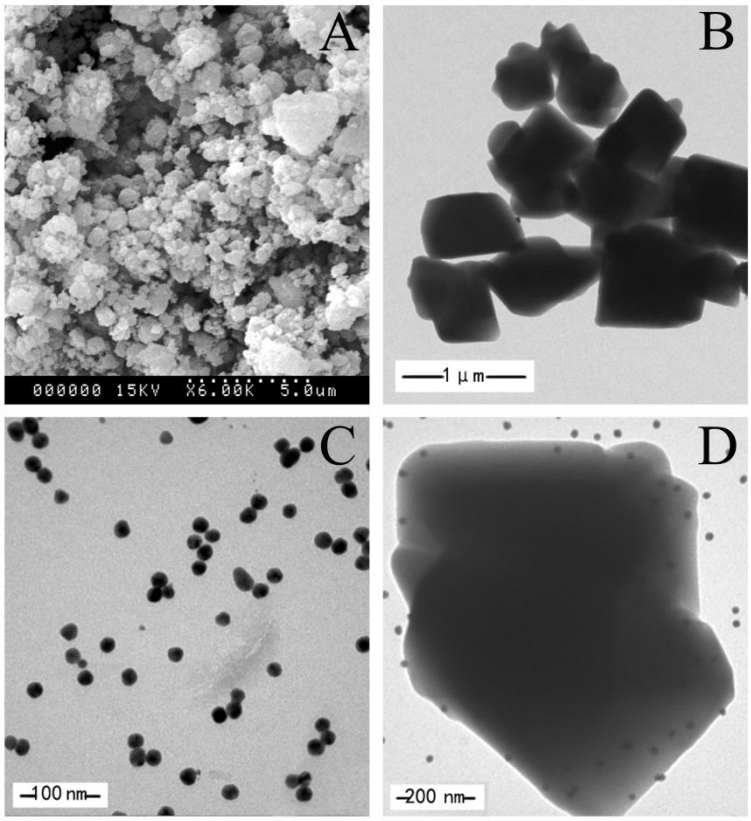

Figure 1. (A) SEM image of the MOF and TEM images of the (B) MOF, (C) AuNPs and (D) MOF/AuNPs.

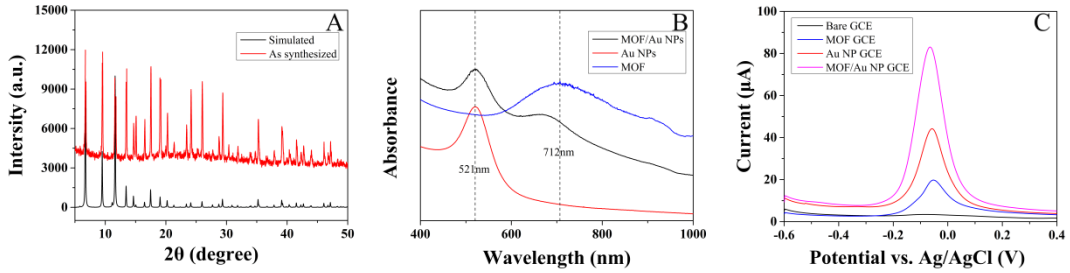

Figure 2. (A) XRD pattern of the MOF; (B) UV–vis spectra of the MOF, AuNPs and MOF/AuNPs; (C) DPV curves of 10 μmol L^{-1} paracetamol on the bare GCE, MOF GCE, AuNP GCE and MOF/AuNP GCE in 0.1 mol L^{-1} phosphate buffer (pH=6).

To compare the electrochemical behaviors of paracetamol for different electrodes, the DPV curves of 10 μmol L−1 paracetamol were investigated on the bare GCE, MOF GCE, AuNP GCE and MOF/AuNP GCE (Fig. 2C). The DPV curve shows a negligible electrochemical signal for paracetamol on the bare GCE. The paracetamol electrochemical signal is observed at −0.06 V on the modified GCEs. The current of the MOF/AuNP GCE was significantly increased. These results may be attributed to the synergistic effect of the MOF and AuNPs. The MOF has a large specific surface area and provides coordinatively unsaturated sites to increase the adsorption amount of paracetamol.

Moreover, the AuNPs exhibit an outstanding electroactivity that accelerates the electron transport, and results in the amplification of the electrochemical signal.

3.2. Detection of paracetamol

Fig. 3A shows the effects of pH on the paracetamol electrochemical response at the MOF/AuNP GCE from pH 4.0 ~ 9.0. The current of paracetamol gradually increased as pH from 4.0 to 6.0. The current decreased with a further increase in the pH because of the participation of the protons. The pH 6 was used to detect paracetamol with the highest sensitivity. Fig. 3B shows that the peak potentials linearly changed upon increasing the pH value. The oxidation potential (E_{pa}) for paracetamol is shown by the following expression [32]:

$$E_{pa}(V)=E_{pa(pH=0)}-(2.303mRT/2F)pH \quad (1)$$

where $E_{pa(pH=0)}$ is the oxidation potential for paracetamol at pH=0, F is Faraday's constant (96485 C mol^{-1}), R=8.314 J·K mol^{-1}, T≈298.15 K, and m is the number of protons involved in the reaction. From Fig. 3B, E_{pa} decreased with a slope of −37.7 mV/pH (R=0.9741). Furthermore, according to dEpa/dpH=−2.303mRT/2F, m was estimated to be approximately 1 in the electrochemical reaction.

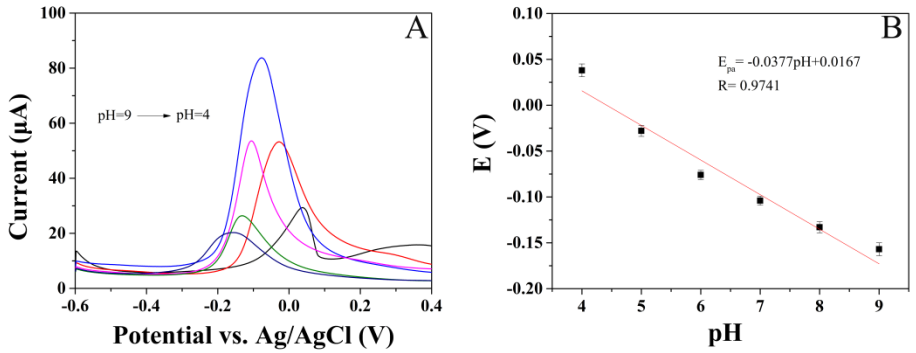

Figure 3. (A) Effects of the pH on the peak current for 10 μmol L^{-1} paracetamol; (B) The linear variation of the peak potential with the increase in the pH.

A critical parameter was the volume of the MOF/AuNP suspension dropped on the GCE surface, and Fig. 4A demonstrates the effects of the amount of the MOF/AuNP dispersion on the peak current. The paracetamol signal increased greatly as the volume increased from 4 to 10 μL. The current decreased gradually with the increase in the cast volume up to 10 μL. It can be explained that excessive MOF/AuNPs may hinder the mass transfer of paracetamol. Therefore, the optimal volume of the MOF/AuNP dispersion was 10 μL.

The effects of the adsorption time were studied in a 10 μmol L^{-1} paracetamol solution by DPV over the range of 30 ~ 150 s (Fig. 4 B). The peak current of paracetamol increased greatly from 30 to 90 s, which indicates that more paracetamol can be adsorbed on the electrode surface. The peak current

maintained a plateau above 90 s, because the adsorption of paracetamol was saturated. In this work, 90 s was selected for the electrochemical experiments.

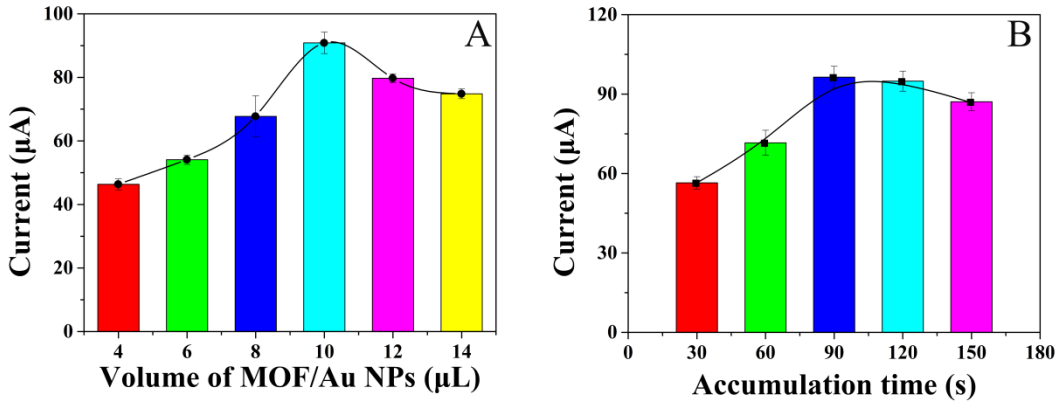

Figure 4. (A) Effects of the MOF/AuNP suspension volumes on the peak current in the presence of 10 μmol L^{-1} paracetamol; (B) Effects of the accumulation time on the peak current in the presence of 10 μmol L^{-1} paracetamol.

3.3. Effects of the scan rates for paracetamol

To reveal the relationship between the scan rate and the electrochemical reaction of paracetamol, the CV curves of the MOF/AuNP GCE were measured in phosphate buffer (0.1 mol L^{-1}, pH=6) containing 10 μmol L^{-1} paracetamol (Fig. 5A). The cathodic (I_{pc}) and anodic (I_{pa}) peak currents increased from 0.025 to 0.6 V s^{-1} (Fig. 5B). The linear equations can be represented as:

I_{pa} (μA)=529.99v (V s^{-1})+50.10 (R=0.9821) (2)

I_{pc} (μA)=−982.66v (V s^{-1})+63.98 (R=0.9934) (3)

Based on the above linear equations, the results indicate an adsorption–controlled quasi−reversible process for paracetamol on the modified electrodes [33].

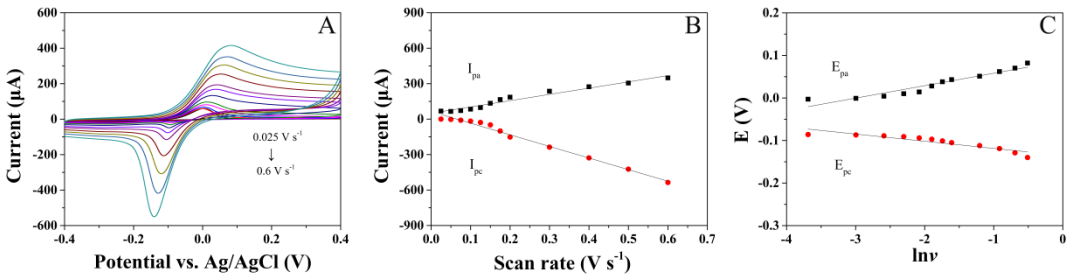

Figure 5. (A) CVs of 10 μmol L^{-1} paracetamol in phosphate buffer (0.1 mol L^{-1}, pH 6) at the following scan rates: 0.025, 0.05, 0.075, 0.1, 0.125, 0.15, 0.175, 0.2, 0.3, 0.4, 0.5 and 0.6 V s^{-1}; (B) the relationship between the peak current and the scan rate, and (C) the relationship between the peak potential and ln$v$.

To investigate the reaction kinetics, the anodic and cathodic (E_{pc}) peak potentials have a linear relationship with the natural logarithm of the scan rate (ln*v*) (Fig. 5C). The linear equations are found to be:

E_{pa} (V)=0.029ln*v* (V s^{-1})−0.087 (R=0. 9586) (4)

E_{pc} (V)=−0.017ln*v* (V s^{-1})−0.135 (R=0. 9170) (5)

The slopes of the E_{pa} and E_{pc} lines can be described as 2.3RT/n(1−α)F and −2.3RT/nαF from Laviron's model [34], respectively. The electron−transfer coefficient (α) was found to be 0.64, and the electron−transfer number (n) was calculated to be 2. According to the above results, the possible paracetamol electrooxidation mechanism on the MOF/AuNP GCE surface was a two−electron and one−proton process. The possible redox mechanism is as follows [8]:

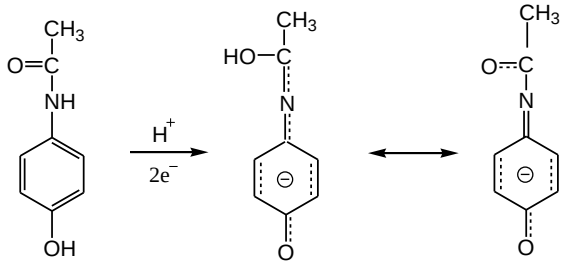

3.4. Reproducibility, stability and interference

The peak currents of five tests were recorded to study the reproducibility of the MOF/AuNP GCE by DPV at a fixed paracetamol concentration of 10 μmol L^{-1}. The relative standard deviation (RSD) was calculated to be 4.29% under the optimized conditions, revealing a satisfactory reproducibility can be obtained by the MOF/AuNP GCE.

To study the stability of the modified GCE, the MOF/AuNP GCE was used to measure 10 μmol L^{-1} paracetamol in phosphate buffer (0.1 mol L^{-1}, pH=6) after being stored in air for four weeks. The oxidation current of paracetamol decreased by only 3.2%, demonstrating the good stability of the MOF/AuNP GCE. This stability facilitates the use of the chemically modified electrode for electroanalytical applications.

To investigate the sensor selectivity, the modified GCE was used to detect paracetamol in the presence of interferents. The detecting signal of 10 μmol L^{-1} paracetamol was individually measured in the presence of 100−fold excess concentrations of ascorbic acid, glucose, lactose, sucrose, urea, K^+, Na^+, SO_4^{2-}, NO_3^- and Cl^- (Fig. 6). The results demonstrated that the potential interfering substances did not interfere with the 10 μmol L^{-1} paracetamol signals, indicating that the present assay offers good sensitivity for determining paracetamol.

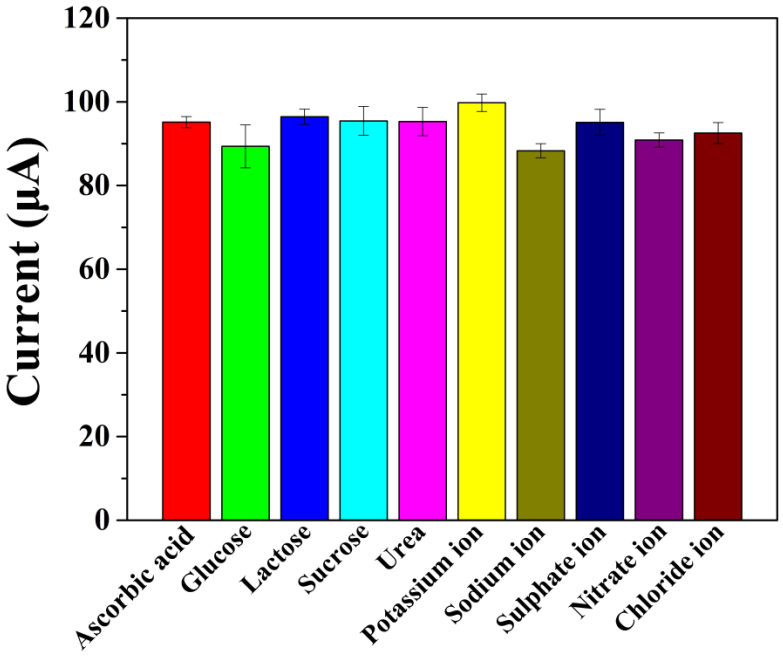

Figure 6. Effects of the presence of organic compounds and inorganic ions on the voltammetric responses of 10 μmol L^{-1} paracetamol using the MOF/AuNP GCE.

3.5. Linear range and LOD

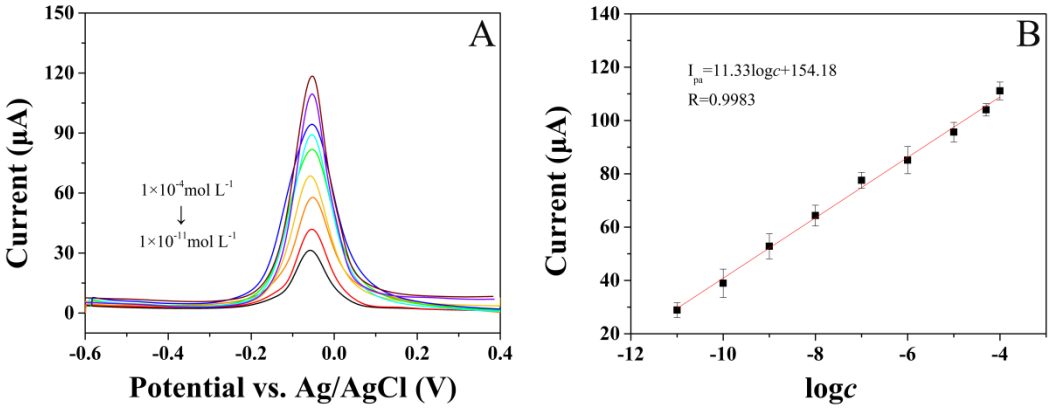

Figure 7. (A) DPV responses for different paracetamol concentrations (1×10^{-11}, 1×10^{-10}, 1×10^{-9}, 1×10^{-8}, 1×10^{-7}, 1×10^{-6}, 1×10^{-5}, 5×10^{-5} and 1×10^{-4} mol L^{-1}) on an MOF/Au NP GCE, and (B) the linear relationship between the peak current and the logarithm of paracetamol concentration.

DPV was utilized to measure the paracetamol peak current on the present electrochemical sensor. The DPV curves of different paracetamol concentrations from 1×10^{-11} mol L^{-1} to 1×10^{-4} mol L^{-1} are shown in Fig. 7A. From Fig. 7B, it can be seen that the paracetamol peak current linearly increased with the addition of paracetamol. The regression equation is I_{pa} (μA)=11.33log*c* (mol

L^{-1})+154.18 (R=0.9983). The LOD was calculated to be approximately 0.0011 nmol L^{-1} as LOD=3σ/S. The detection limit of the MOF/AuNP GCE was lower than previous reports using electrochemical method for detecting paracetamol. The comparison is shown in Table 1.

Table 1. Comparison of different electrochemical methods for determination of paracetamol.

Electrode	Linear range (nmol L^{-1})	Detection Limit (nmol L^{-1})	Reference
Graphene/ GCE	100–20,000	32	[8]
CNB/GC	80–2,300,000	8	[9]
CoNPs/MWCNT/GCE	5.2–450	1	[10]
MWCNTs/GCE	0.2–15,000	0.09	[11]
MWCNTs/CTS–Cu/GCE	100–200,000	24	[35]
MIP/pABSA/GCE	50–100,000	43	[36]
Pd/GO/GCE	5–50	2.2	[37]
MOF/AuNPs/Nafion/GCE	0.01–100,000	0.0011	This work

3.6. Real sample analysis

Table 2. Determination of paracetamol in commercial tablets.

Samples	Declared (mg/tablet)	Present method			HPLC		
		Found (mg/tablet)	RSD (%, n=3)	Recovery (%)	Found (mg/tablet)	RSD (%, n=3)	Recovery (%)
1	325	331	3.13	101.7	329	3.15	101.1
2	325	334	2.85	102.9	331	2.55	101.9
3	325	332	2.32	102.1	331	2.89	101.8
4	325	330	2.99	101.4	333	3.24	102.5

The present method was used to detect paracetamol in real samples. The commercial tablet (produced in Shanghai, China) with a nominal value of 325 mg was used for the analysis of paracetamol. A commercial paracetamol tablet was crushed and 20 mL of ethanol was added. After ultrasonication for 10 min, the dispersion was filtered. The filtrate was extracted three times with ethanol. All filtrates were collected and diluted in a 50-mL flask with ethanol. The sample solution (0.1 mL) was diluted 1, 000 times with ethanol. The sample (100 μL) was added to 10.0 mL of phosphate buffer (pH 6.0) and detected by the present sensor. Table 2 shows that the content of paracetamol is 330 ~ 334 mg per tablet. There is a good agreement with the label amount (325 mg) with recoveries of 101.4 ~ 102.9%. The paracetamol content was also evaluated by HPLC measurement. The contents of the assayed tablets agrees well with the content of paracetamol on the label of the pharmaceutical

products, suggesting that the MOF/AuNP sensor is suitable for paracetamol determination with high sensitivity and precision.

4. CONCLUSION

A water–stable MOF with a large specific surface area was synthesized and has potential opportunities for use in the electrochemical field. As we all know, AuNPs possess outstanding electrical conductivity and have been used to solve problems in electrochemical applications. The MOF/AuNP composites amplified an electrochemical signal because of the synergistic effect of the MOF and the AuNPs. The modified electrode demonstrated the sensitive measurement of paracetamol with an LOD of 0.0011 nmol L^{-1}. Furthermore, the MOF/AuNP GCE can be used to determining paracetamol in tablet samples. The study of paracetamol electrochemical detection offers a platform for broadening the application of MOF composites in electroanalysis, which is an excellent electrochemical method for pharmaceutical analysis.

ACKNOWLEDGMENTS
This work was supported by Program for Key Science and Technology Innovation Team in Shaanxi Province (No. 2014KCT−27).

References

1. K. Allegaert, J.N. van den Anker, *Semin. Fetal Neonat. M.*, 22 (2017) 308.
2. G. Fan, B. Wang, C. Liu, D. Li, *Allergol. Immunopath.*, 45 (2017) 528.
3. I.C. Guiloski, J.L.C. Ribas, L.D.S. Piancini, A.C. Dagostim, *Environ. Toxicol. Phar.*, 53 (2017) 111.
4. Z.A. ALOthman, M.A. Abdalla, *Arab. J. Chem.*, 4 (2011) 239.
5. A. Klimek−Turek, M. Sikora, M. Rybicki, T.H. Dzido, *J. Chromatogr. A*, 1436 (2016) 19.
6. S. Glavanović, M. Glavanović, V. Tomišić, *Spectrochim. Acta A*, 157 (2016) 158.
7. T. Hložek, T. Křížek, P. Tůma, M. Bursová, *J. Pharmaceut. Biomed.*, 145 (2017) 616.
8. X. Kang, J. Wang, H. Wu, J. Liu, I.A. Aksay, Y.H. Lin, *Talanta*, 81 (2010) 754.
9. P.A. Raymundo−Pereira, A.M. Campos, C.D. Mendonça, M.L. Calegaro, *Sensor. Actuat. B Chem.*, 252 (2017) 165.
10. A. Kutluay, M. Aslanoglu, *Anal. Chim. Acta*, 839 (2014) 59.
11. J. Li, J. Liu, G.Tan, J. Jiang, S. Peng, *Biosens. Bioelectron.*, 54 (2014) 468.
12. H. Zhou, S. Kitagawa, *Chem. Soc. Rev.*, 43 (2014) 5415.
13. J.J. Alcañiz, R. Gielisse, A.B. Lago, E.V.R. Fernandez, *Catal. Sci. Technol.*, 3 (2013) 2311.
14. M. Deng, S. Lin, X. Bo, L. Guo, *Talanta*, 174 (2017) 527.
15. Q. Chen, X. Li, X. Min, D. Cheng, *J. Electroanal. Chem.*, 789 (2017) 114.
16. A. Morozan, F. Jaouen, *Energy Environ. Sci.*, 5 (2012) 9269.
17. M.C. Daniel, D. Astruc, *Chem. Rev.*, 104 (2004) 293.
18. P. Priecel, H.A. Salami, R.H. Padilla, Z.Y. Zhong, *Chinese J. Catal.*, 37 (2016) 1619.
19. X. Tian, C. Cheng, H. Yuan, J. Du, *Talanta*, 93 (2012) 79.
20. R. Mossanha, C.A. Erdmann, C.S. Santos, K. Wohnrath, S.T. Fujiwara, C.A. Pessoa, *Sensor. Actuat. B Chem.*, 252 (2017) 747.
21. D. Peng, R. Liang, H. Huang, J. Qiu, *J. Electroanal. Chem.*, 761 (2016) 112.

22. H. Zhai, H. Wang, S. Wang, Z. Chen, S. Wang, Q. Zhou, Y. Pan, *Sensor. Actuat. B Chem.*, 255 (2018) 1771.
23. C.T.P. da Silva, F.R. Veregue, L.W. Aguiar, J.G. Meneguin, M.P. Moisés, *New J. Chem.*, 40 (2016) 8872.
24. H. Hosseini, H. Ahmar, A. Dehghani, A. Bagheri, A. R. Fakhari, M.M. Amini, *Electrochim. Acta*, 88 (2013) 301.
25. Z. Wei, S. Chan, L. Li, H. Cai, *Electrochim. Acta*, 50 (2005) 2279.
26. H. Chen, L. Wang, J. Yang, R. Yang, *J. Phys. Chem. C*, 117 (2013) 7565.
27. L. Liu, X. Wang, J. Yang, Y. Bai, *Anal. Biochem.*, 535 (2017) 19.
28. X. Yang, Y. Zhang, *Catal. Commun.*, 94 (2017) 9.
29. S.S.Y Chui, S.M.F. Lo, J.P.H. Chamant, A.G. Orpen, I.D. Williams, *Science*, 283 (1999) 1148.
30. A.R. Abbasi, M. Karimi, M.Y. Masoomi, *Colloid. Surface A*, 520 (2017) 193.
31. K. Magyari, T. Nagy−Simon, A. Vulpoi, R.A. Popescu, E. Licarete, R. Stefan, K. Hernádi, I. Papuc, L. Baia, *Mat. Sci. Eng. C−Mater.*, 76 (2017) 752.
32. A. Afkhami, D. Nematollahi, L. Khalafi, M. Rafiee, *Int. J. Chem. Kinet*, 37 (2005) 17.
33. K. Liu, J. Wei, C. Wang, *Electrochim. Acta*, 56 (2011) 5189.
34. E. Laviron, *J. Electroanal. Chem.*, 101 (1979) 19.
35. A. Mao, H. Li, D. Jin, L. Yu, X. Hu, *Talanta*, 144 (2015) 252.
36. Y. Teng, L. Fan, Y. Dai, M. Zhong, X. Lu, X. Kan, *Biosens. Bioelectron.*, 71 (2015) 137.
37. A. Kutluay, M. Aslanoglu, *Sensor. Actuat. B Chem.*, 185 (2013) 398.